THE
PHYSICAL REVIEW

A journal of experimental and theoretical physics established by E. L. Nichols in 1893

SECOND SERIES, Vol. 140, No. 1A 4 OCTOBER 1965

Influence of Screening on the Atomic Photoeffect*†

J. J. MATESE AND W. R. JOHNSON
University of Notre Dame, Notre Dame, Indiana
(Received 13 May 1965)

The atomic photoeffect in a screened Coulomb field is considered. Numerical calculations of the differential and total cross sections for the K and L shells are given. Screening is introduced by including an exponential damping term in the potential. The bound-state wave function and the screening parameter λ are determined by using a variational technique to fit the experimental ionization energy of the shell under consideration. The continuum electron is described by a partial-wave decomposition, and the interaction with the radiation field is treated in lowest order perturbation theory. A numerical program is developed to obtain the radial part of the continuum wave function. The cross sections are computed numerically and corrections to pure-Coulomb-field results are found to be small for the K shell but significant for the L shell. Results for $\lambda=0$ are obtained and found to be in good agreement with previous theoretical work. This serves as a check on the accuracy of the numerical computations. A separate calculation using relativistic Hartree wave functions and potentials is carried out for mercury. Comparison of the results of this test calculation with the simplified exponential model indicates that the effects of screening are accounted for reasonably well by the model.

I. INTRODUCTION

RECENTLY detailed numerical calculations of differential and total cross sections for the atomic photoeffect were reported by Pratt *et al.*,[1] who considered the K shell using an unscreened Coulomb potential. These K-shell results were found to be in good agreement with previous calculations and with experiments. Alling and Johnson[2] have extended the work done in this field to the L shell and have found some discrepancies with the scant experimental data available for this shell. These discrepancies were assumed to be the result of the neglect of screening, which should modify the L-shell cross sections significantly. The calculations done here, which cover nuclei and photon energies of possible future experimental interest, give quantitative predictions of the effect of screening on the photoeffect. For the sake of simplicity we restrict our consideration to central-field potentials, in particular to those of the form $V(r)=-(\alpha Z/r)e^{-\lambda r}$. The limit $\lambda\rightarrow 0$ affords a check of our results with previous pure-Coulomb-potential calculations. We assume that the bound-state and continuum electrons interact only with the screened potential. Section II will include a development of the general formalism. In Sec. III a discussion is made of the numerical procedures used to evaluate the screening parameters, wave functions, phase shifts, and radial integrals. Programs to determine these quantities were written for the Notre Dame UNIVAC-1107 computer. These programs were constructed so that either the screened or the unscreened cross section could be evaluated by simply changing parameters. Because of this simple check an extensive error analysis will not be given. The new results for the screened Coulomb field are presented in Sec. IV where comparisons with experiment and with the unscreened calculations are made. The calculations cover the energy region 81 to 1332 keV and include $Z=47$, 82, and 92.

A calculation using relativistic Hartree wave functions and potentials for mercury, $Z=80$, with an energy of 354 keV is also presented in Sec. IV.

* This work was supported in part by the U. S. Atomic Energy Commission.

† Based on a doctoral dissertation submitted by one of us (J.J.M.) to the Department of Physics, University of Notre Dame, Notre Dame, Indiana.

[1] R. H. Pratt, R. D. Levee, R. L. Pexton, and W. Aron, Phys. Rev. **134**, A898 (1964). Another numerical calculation has been done by S. Hultberg, B. Nagel, and P. Olsson, Arkiv Fysik **20**, 555 (1961).

[2] W. R. Alling and W. R. Johnson (to be published). The relativistic L-shell Born approximation is given by M. Gavrila, Phys. Rev. **124**, 1132 (1961).

II. GENERAL FORMALISM

A standard partial-wave decomposition of the photoelectric amplitude for both the K and L shells is carried out below. The K shell expansion is essentially identical with that obtained by Pratt *et al.*[1] We consider an incident photon of energy ω interacting with an electron bound in a spherically symmetric central field. The radiation interaction is treated in lowest order perturbation theory; thus we neglect effects of relative order $\alpha=1/137$. All relativistic effects are included by treating the interactions of the bound-state and continuum electrons with the potential in an exact manner. We write our differential cross section in the form[3]

$$\frac{d\sigma}{d\Omega}=\frac{\alpha}{2\pi}\frac{pW}{\omega}\tfrac{1}{2}\sum|M_{fi}|^2 \tag{1}$$

with

$$M_{fi}=\int d\mathbf{r}\psi_f^{\dagger}\boldsymbol{\alpha}\cdot\hat{\boldsymbol{\epsilon}}e^{i\mathbf{k}\cdot\mathbf{r}}\psi_i, \tag{2}$$

where $(\mathbf{p},iW)$ = four-momentum of final electron, $(\mathbf{k},i\omega)$ = four-momentum of incident electron,

$$\boldsymbol{\alpha}=\begin{pmatrix}0 & \boldsymbol{\sigma}\\ \boldsymbol{\sigma} & 0\end{pmatrix},$$

$\boldsymbol{\sigma}$ being the Pauli spin matrices, and $\hat{\boldsymbol{\epsilon}}$ a unit vector specifying the polarization direction of the incident photon. We will consider the incident photon beam to be unpolarized and will count all electrons coming out, regardless of their spins. Therefore we must average over polarization directions and sum over final electron spins. Since we are interested in the cross section for a particular shell or subshell we sum over all electrons in the shell under consideration. In Eq. (1), $\sum$ represents the polarization and spin sums. The wave function ψ_i describes the bound-state electrons of energy $W_B<1$ and $\psi_f^{\dagger}$ represents the Hermitian adjoint of the continuum wave function ψ_f which is a solution to Dirac's equation for energy $W>1$ having the asymptotic form of a plane wave plus an incoming spherical wave. The continuum wave function is written as a sum over partial waves.

In the sequel we will use zero subscripts to denote the bound state and barred subscripts for the radiation field. Quantities without subscripts refer to the continuum.

The bound-state wave function is given by

$$\psi_i=\begin{pmatrix}ig_{x_0}\Omega_{x_0m_0}\\ f_{x_0}\Omega_{-x_0m_0}\end{pmatrix}, \tag{3}$$

where

$$\Omega_{xm}=\begin{pmatrix}C_{xm}{}^{+}Y_{l,m-\frac{1}{2}}\\ C_{xm}{}^{-}Y_{l,m+\frac{1}{2}}\end{pmatrix} \tag{4}$$

with

$$\begin{aligned}C_{xm}{}^{+}&=C(l\tfrac{1}{2}j;m-\tfrac{1}{2},\tfrac{1}{2})=-\eta_x\left[\frac{\eta_x(x+\frac{1}{2}-m)}{2l+1}\right]^{1/2},\\ C_{xm}{}^{-}&=C(l\tfrac{1}{2}j;m+\tfrac{1}{2},-\tfrac{1}{2})=\left[\frac{\eta_x(x+\frac{1}{2}+m)}{2l+1}\right]^{1/2}.\end{aligned} \tag{5}$$

The symbol $C(l_1l_2l_3;m_1m_2)$ denotes the Clebsch-Gordan coefficient as defined by Rose.[4] Throughout we use the following notation, giving the angular-momentum quantum numbers as functions of x:

$$\begin{aligned}&l=x, && j=l-\tfrac{1}{2} \quad \text{for} \quad x>0,\\ &l=-x-1, && j=l+\tfrac{1}{2} \quad \text{for} \quad x<0.\end{aligned} \tag{6}$$

We will also use $l'(x)=l(-x)$, $k=|x|$, $\eta_x=x/k$. The wave function is normalized by requiring that

$$\int_0^{\infty}r^2dr(f_{x_0}{}^2+g_{x_0}{}^2)=1. \tag{7}$$

Our continuum is described by

$$\psi_f=4\pi\sum_{xm}(\Omega^{\dagger}{}_{xm}(\hat{p}),v)e^{-i\delta_x}\begin{pmatrix}ig_x\Omega_{xm}(\hat{r})\\ f_x\Omega_{-xm}(\hat{r})\end{pmatrix}, \tag{8}$$

where v is the large component of the plane-wave spinor and the x sum runs over all nonzero integers. The radial functions are normalized such that

$$\begin{aligned}g_x&\xrightarrow[r\to\infty]{}\left[\frac{W+1}{2W}\right]^{1/2}\frac{1}{pr}\cos(pr+\delta_x),\\ f_x&\xrightarrow[r\to\infty]{}\left[\frac{W-1}{2W}\right]^{1/2}\frac{1}{pr}\sin(pr+\delta_x).\end{aligned} \tag{9}$$

Choosing $\mathbf{k}$ along the z axis the retardation factor of the radiation field may be expanded as

$$e^{i\mathbf{k}\cdot\mathbf{r}}=\sum_{\bar{l}}(2\bar{l}+1)i^{\bar{l}}j_{\bar{l}}(\omega r)P_{\bar{l}}(\cos\theta), \tag{10}$$

where $j_{\bar{l}}(\omega r)$ is a spherical Bessel function of order $\bar{l}$.

The angular integration in Eq. (2) is straightforward when expressions (3), (8), and (10) are used. The matrix element can then be expressed in terms of the radial integrals

$$\begin{aligned}I_{xx_0\bar{l}}&=i^{\bar{l}}\int_0^{\infty}r^2drj_{\bar{l}}(\omega r)g_x{}^{*}(pr)f_{x_0}(r),\\ J_{xx_0\bar{l}}&=i^{\bar{l}}\int_0^{\infty}r^2drj_{\bar{l}}(\omega r)f_x{}^{*}(pr)g_{x_0}(r).\end{aligned} \tag{11}$$

[3] We use natural units $\hbar=m_e=c=1$.

[4] M. E. Rose, *Elementary Theory of Angular Momentum* (John Wiley & Sons, Inc., New York, 1957). His spherical harmonics are used as well.

TABLE I. Bound-state wave-function parameters for Coulomb potential.

Shell	γ	W_B	μ	a_0	a_1	c_0	c_1	N
K	$(1-\alpha^2Z^2)^{1/2}$	γ	αZ	1	0	1	0	$\left(\frac{\mu}{\Gamma(2\gamma+1)}\right)^{1/2}$
L_{I}	$(1-\alpha^2Z^2)^{1/2}$	$\left(\frac{1+\gamma}{2}\right)^{1/2}$	$\frac{\alpha Z}{2W_B}$	$2W_B^2+W_B-1$	μ	$W_B(2W_B-1)$	μ	$\left(\frac{\mu}{W_B(2W_B-1)\Gamma(2\gamma+1)}\right)^{1/2}$
L_{II}	$(1-\alpha^2Z^2)^{1/2}$	$\left(\frac{1+\gamma}{2}\right)^{1/2}$	$\frac{\alpha Z}{2W_B}$	$W_B(2W_B+1)$	μ	$2W_B^2-W_B-1$	μ	$\left(\frac{\mu}{W_B(2W_B+1)\Gamma(2\gamma+1)}\right)^{1/2}$
L_{III}	$(4-\alpha^2Z^2)^{1/2}$	$\frac{\gamma}{2}$	$\frac{\alpha Z}{2}$	1	0	1	0	$\left(\frac{\mu}{\Gamma(2\gamma+1)}\right)^{1/2}$

When the spin and polarization sums are done in Eq. (1) the differential cross section can be written in the compact form

$$\frac{d\sigma}{d\Omega}=4\alpha\frac{pW}{\omega}\sum_{m_0}\left[|F_{m_0}(\theta)|^2+|G_{m_0}(\theta)|^2\right], \tag{12}$$

where

$$F_{m_0}(\theta)=\sum_x\frac{1}{k}\left[\delta_{m_0,-\frac{3}{2}}+x^2\delta_{m_0,-\frac{1}{2}}+x(x-1)\delta_{m_0,\frac{1}{2}}+x(x-2)\delta_{m_0,\frac{3}{2}}\right]e^{i\delta_x}Q_x(m_0)P_l^{m_0+\frac{1}{2}}(\cos\theta), \tag{13}$$

$$G_{m_0}(\theta)=\sum_x\eta_x e^{i\delta_x}Q_x(m_0)P_l^{m_0+\frac{1}{2}}(\cos\theta).$$

Explicit expressions for the Q's in terms of the radial integrals I and J are given for the K and L shells in the Appendix. Equations (13) as given are valid only for these shells. All Q's not given are zero due to selection rules. Using this notation we finally arrive at the remarkably simple expression for the total cross section

$$\sigma_T=16\pi\alpha\frac{pW}{\omega}\sum_x\frac{1}{k}\left[|Q_x(-\tfrac{3}{2})|^2+k^2|Q_x(-\tfrac{1}{2})|^2+k^2(k^2-1)|Q_x(\tfrac{1}{2})|^2+k^2(k^2-1)(k^2-4)|Q_x(\tfrac{3}{2})|^2\right]. \tag{14}$$

III. NUMERICAL EVALUATION OF THE RADIAL INTEGRALS

The problem is essentially completed once the various radial integrals I and J are computed and the phase shifts δ_x are found. In Pratt's work[1] the bound-state and continuum radial wave functions were determined numerically. Alling and Johnson[2] were able to solve analytically for the radial integrals using well-known expressions for the wave functions. It is necessary here to treat the entire problem numerically because of the lack of analytic solutions for screened potentials. The discussion of this work will be separated into three parts covering the bound state, continuum, and radial integral problems.

(A) The Bound State

The bound-state radial functions are solutions to Dirac's radial equations

$$\frac{d}{dr}\begin{pmatrix}G_{x_0}(r)\\F_{x_0}(r)\end{pmatrix}+\begin{pmatrix}x_0/r & 1+W_B-V(r)\\1-W_B+V(r) & -(x_0/r)\end{pmatrix}\times\begin{pmatrix}G_{x_0}(r)\\F_{x_0}(r)\end{pmatrix}=0, \tag{15}$$

where

$$G_{x_0}(r)=rg_{x_0}(r),\quad F_{x_0}(r)=rf_{x_0}(r). \tag{16}$$

The solutions for the K and L shells in a pure Coulomb potential $V(r)=-\alpha Z/r$ are well known and of the form[5]

$$\begin{aligned}G_{x_0}(r)&=N(1+W_B)^{1/2}(2\mu r)^\gamma e^{-\mu r}(c_0-c_1r),\\F_{x_0}(r)&=N(1-W_B)^{1/2}(2\mu r)^\gamma e^{-\mu r}(a_0-a_1r),\end{aligned} \tag{17}$$

where the values of the parameters are given in Table I.

To introduce screening into the photoelectric problem one chooses a model for the potential and solves for the bound-state wave functions numerically. Unessential mathematical difficulties are avoided by using an exponentially damped Coulomb potential

$$V(r)=-(\alpha Z/r)e^{-\lambda r}. \tag{18}$$

The parameter λ is chosen so that computed values of ionization energies

$$I_B=1-W_B \tag{19}$$

agree with the experimental energies tabulated in Hill, Church, and Mihelich.[6] Since photoelectric cross sections are very sensitive to I_B, any screening model must reproduce its experimental value to yield reliable results. We choose the bound-state wave functions to have the same functional form as Eqs. (17), but treat

[5] M. E. Rose, *Relativistic Electron Theory* (John Wiley & Sons, Inc., New York, 1961), p. 179. A different phase convention for the radial wave functions is adopted here.

[6] R. D. Hill, E. L. Church, and J. W. Mihelich, Rev. Mod. Phys. **10**, 523 (1952).

TABLE II. Screening parameters λ computed using the variational method to fit experimental binding energies compared with the Fermi-Thomas parameter $\lambda=1.12\alpha Z^{1/3}$.

Z	K	L_{I}	L_{II}	L_{III}	Fermi-Thomas
92	0.0527	0.0421	0.0438	0.0421	0.0369
82	0.0468	0.0393	0.0407	0.0396	0.0355
47	0.0333	0.0286	0.0296	0.0294	0.0295

μ and γ as variational parameters. The coefficients N, W_B, c_0, c_1, a_0, and a_1 are then given as functions of μ and γ according to Table I.

The expectation value of the ionization energy is given by

$$\langle I_B\rangle=1-\int_0^\infty dr\begin{pmatrix}G_{x_0}(r)\\F_{x_0}(r)\end{pmatrix}^{\dagger}H(r)\begin{pmatrix}G_{x_0}(r)\\F_{x_0}(r)\end{pmatrix}, \tag{20}$$

where $H(r)$ is the radial Hamiltonian for the bound state with $V(r)$ given by Eq. (18). The integral in (20) is done analytically and gives the binding energy as a function of the two variational parameters μ and γ and the screening parameter λ. The variations of $\langle I_B\rangle$ with respect to μ and γ give the following three nonlinear equations

$$\begin{aligned}&\langle I_B\rangle=I_B\ (\text{experimental}),\\&\partial\langle I_B\rangle/\partial\mu=0,\\&\partial\langle I_B\rangle/\partial\gamma=0,\end{aligned} \tag{21}$$

which are solved numerically using a repeating linear interpolation approximation until all three parameters have converged to within 1 part in 10^6. The remaining coefficients are obtained by using Table I. Various other parameterizations were considered; all yielded screening parameters which agreed to within 1 part in 10^3. Table II gives a list of the values of λ used in evaluating the K- and L-shell cross sections. The Fermi-Thomas parameter

$$\lambda_{\mathrm{FT}}=1.12\alpha Z^{1/3} \tag{22}$$

is included for comparison. Table III includes a representative set of numerically computed parameters and compares them with the corresponding values for the pure-Coulomb-field parameters.

TABLE III. The bound-state parameters μ and W_B defined in Table I for $Z=82$. The experimental $1-I_B$ would equal W_B (Coulomb) if screening effects were not significant in lead.

Shell	Numerical μ	Coulomb μ	Numerical W_B	Coulomb W_B	Experimental $1-I_B$
K	0.5970	0.5984	0.8025	0.8012	0.8279
L_{I}	0.3080	0.3153	0.9522	0.9490	0.9690
L_{II}	0.3081	0.3153	0.9519	0.9490	0.9703
L_{III}	0.2893	0.2992	0.9573	0.9542	0.9745

(B) The Continuum State

The continuum radial functions are also solutions to Eqs. (15) with W_B replaced by $W=1+\omega-I_B(\text{expt.})$; they are normalized according to Eqs. (9). The procedure used for solving this set of coupled equations is to integrate them numerically to a point r_0 chosen so large that the potential is negligible. At this point the radial functions are matched to free-field solutions using the relations

$$\begin{aligned}g_x(pr_0)&=[(W+1)/2W]^{1/2}(Aj_x(pr_0)-Bn_x(pr_0)),\\f_x(pr_0)&=-[(W-1)/2W]^{1/2}\\&\quad\times(Aj_{x-1}(pr_0)-Bn_{x-1}(pr_0)),\end{aligned} \tag{23}$$

where j_x and n_x are spherical Bessel functions. The coefficients A and B are determined by the matching procedure. If we let

$$\begin{aligned}A&=C\cos[\delta_x+\tfrac{1}{2}(x+1)\pi],\\B&=C\sin[\delta_x+\tfrac{1}{2}(x+1)\pi],\end{aligned} \tag{24}$$

the asymptotic solutions are

$$\begin{aligned}g_x(pr)&\underset{r\to\infty}{\longrightarrow}[(W+1)/2W]^{1/2}(C/pr)\cos(pr+\delta_x),\\f_x(pr)&\underset{r\to\infty}{\longrightarrow}[(W-1)/2W]^{1/2}(C/pr)\sin(pr+\delta_x).\end{aligned} \tag{25}$$

In order to investigate the errors introduced by matching at the point r_0 we consider a transformation given by Rose[7]

$$\begin{aligned}g_x(pr)&=[(W+1)/2W]^{1/2}(\tilde{C}(r)/pr)\cos(pr+\tilde{\delta}_x(r)),\\f_x(pr)&=[(W-1)/2W]^{1/2}(\tilde{C}(r)/pr)\sin(pr+\tilde{\delta}_x(r)).\end{aligned} \tag{26}$$

Using (26), the radial equations (15) can be rewritten

$$\begin{aligned}\frac{1}{\tilde{C}}\frac{d\tilde{C}}{dr}&=-\frac{x}{r}\cos 2(pr+\tilde{\delta}_x)+\frac{\alpha Z}{pr}e^{-\lambda r}\sin 2(pr+\tilde{\delta}_x),\\\frac{d\tilde{\delta}_x}{dr}&=-\frac{x}{r}\sin 2(pr+\tilde{\delta}_x)+\frac{\alpha Z}{pr}e^{-\lambda r}[W+\cos 2(pr+\tilde{\delta}_x)].\end{aligned} \tag{15'}$$

When these equations are matched to free-field solutions at r_0 one sees that oscillations of the order

$$\Delta C/C\approx(\alpha Z/pr_0)e^{-\lambda r_0},\quad \Delta\delta_x\approx(\alpha Z/pr_0)e^{-\lambda r_0}(W+1) \tag{27}$$

TABLE IV. Unscreened L_{II} shell total cross sections in barns for uranium. (1) Present work, (2) Alling and Johnson (Ref. 2).

ω (keV)	(1)	(2)
81	320.2	322.6
103	163.8	162.6
279	9.704	9.710
354	5.103	5.102
412	3.420	3.422
663	1.055	1.055
1332	0.236	0.236

[7] M. E. Rose, Phys. Rev. **82**, 470 (1951).

TABLE V. K- and L-shell total cross sections in barns for uranium. (1) Present work with screening, (2) Pratt *et al.* (Ref. 1) without screening, (3) Alling and Johnson (Ref. 2) without screening.

	K shell		L_{I} shell		L_{II} shell		L_{III} shell	
ω (keV)	(1)	(2)	(1)	(3)	(1)	(3)	(1)	(3)
81	...	...	367.3	382.4	300.3	322.6	263.2	297.6
103	...	...	208.5	219.0	150.1	162.6	122.3	139.4
135	...	...	108.7	...	68.58	...	51.56	...
167	...	...	64.65	...	37.11	...	26.25	...
208	...	...	37.74	...	19.80	...	13.19	...
279	153.1	155.	18.44	19.86	8.675	9.710	5.357	6.213
354	84.99	...	10.43	11.25	4.528	5.102	2.647	3.070
412	58.99	59.9	7.302	7.891	3.024	3.422	1.711	1.984
662	20.04	20.4	2.520	2.727	0.923	1.055	0.481	0.555
1000	8.501	...	1.071	...	0.365	...	0.180	...
1332	4.884	4.93	0.614	0.665	0.205	0.236	0.098	0.112

are being neglected. For the results quoted here r_0 was chosen equal to 120. The worst errors that arise in the screened calculations are for the L shell with $\omega=81$ keV, $Z=47$ in which case the oscillations are of the order of 1 part in 10^4.

To integrate the continuum functions out to r_0, the coupled first-order equations (15) were reduced to two second-order uncoupled equations. A fixed-interval, five-point integration procedure given by Kopal[8] was used with step size h. His analysis for error propagation indicates that the integration be started at a point $r_j=jh$, where $j\geqslant k$, in order that errors be bounded. In fact $j=2k$ was used here. A power series was developed to take the wave functions from $r=0$ to $r=r_j$. Step sizes of $h=0.0625$ and 0.125 are considered. The disagreement in results for the two step sizes is less than the errors introduced by the fitting process at r_0. For this reason $h=0.125$ is used in results quoted here.

(C) The Radial Integrals

The radial integrals I and J are evaluated using Simpson's rule with step size h. Contributions beyond $\mu r=20$ are neglected since the bound-state wave function has decreased by a factor of at least 10^{-7} from its maximum value. The two step sizes were used in selected cases and yield results which agree to four significant figures up to an energy of 412 keV. Agreement deteriorated somewhat at higher energies. The Bessel functions used were generated in double precision using the method of Corbato and Uretsky.[9]

IV. RESULTS

(A) Theoretical Comparisons

Table IV includes L_{II}-shell total cross sections for $\lambda=0$, $Z=92$, and compares them with the results of Alling and Johnson.[2] The disagreement is largest at small photon energies and vanishes at higher energies. This can be attributed to the fact that the oscillations referred to in Eq. (32) are not negligible for $\lambda=0$ and small electron momentum. However, when λ is not equal to zero we can expect such discrepancies to disappear. In addition, the agreement of results at high energies implies that the integration mesh is fine enough to yield at least three significant figures for the screened cross sections given here. Results for the unscreened K, L_{I}, and L_{III} shells show much the same agreement with previous computations.[1,2]

Table V compares K- and L-shell total cross sections with screening to previous unscreened calculations for uranium. One notices that screening uniformly decreases the total cross section. Percent reductions are relatively independent of energy for the range considered and are of the order of 1, 7, 11, and 14% for the K, L_{I}, L_{II}, and L_{III} shells of uranium.

Table VI lists new results for silver ($Z=47$) and lead ($Z=82$). Percent reductions for these nuclei are approximately 2, 25, 32, and 28%, for the K, L_{I}, L_{II}, and L_{III} shells of silver and 1, 10, 15, and 16% for the K, L_{I}, L_{II}, and L_{III} shells of lead.

The new results indicate that K-shell screening is negligible as had been anticipated. L-shell screening

TABLE VI. Screened total cross sections in barns for the K and L shells of lead and silver.

	$Z=82$				$Z=47$			
ω (keV)	K	L_{I}	L_{II}	L_{III}	K	L_{I}	L_{II}	L_{III}
81	...	256.7	149.3	146.4	...	32.13	4.602	6.537
103	...	142.1	72.25	66.89	...	16.33	2.006	2.783
279	99.95	11.46	3.737	2.774	10.21	0.974	0.072	0.093
354	54.40	6.354	1.910	1.360	5.283	0.510	0.034	0.044

[8] Z. Kopal, *Numerical Analysis* (Chapman and Hall Ltd., London, 1961), Sec. IV-K.
[9] F. J. Corbato and J. L. Uretsky, J. Assoc. Comp. Mach. **6**, 366 (1959).

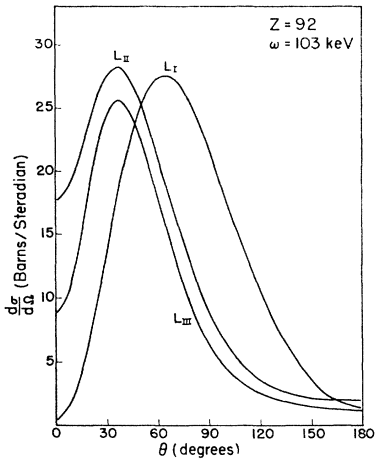

FIG. 1. Calculations of L-shell angular distributions for uranium $Z=92$ and photon energy $\omega=103$ keV.

effects become more important for low-Z elements. This can be explained by the fact that the inner-electron screening reduces the nuclear charge seeen by L-shell electrons. This reduction is relatively independent of Z and therefore yields a larger percent effect for low-Z elements.

With one exception screening effects increase slightly as one progresses through the L shells. This is a reflection of the fact that the mean radius of the bound-state electron increases slightly in going from L_{I} to L_{III} and therefore a small increase in the effect of screening is expected.

(B) Comparison with Experiment

(i) *Angular Distributions*

Experimental K-shell angular distributions have been obtained for uranium by Hultberg[10] at 412, 662, and 1332 keV and Sujkowski[11] at 279 keV. Sujkowski's result is in good agreement with unscreened calculations except at forward angles where his result is too large. The present work does not indicate any significant changes in K-shell angular distributions.

Uncorrected L-shell angular distributions have been obtained by Sujkowski[11] for uranium at a photon energy of 103 keV. Figure 1 shows the present results for this case. In general screening does not affect the shape of the angular distribution. Roughly there is a uniform percentage reduction in the angular distribution from 0° to 180°.

(ii) *Total Cross Sections*

Colgate[12] has measured total cross sections for the K shell of uranium. His results are 58.6, 19.9, and 4.7 b for photon energies of 412, 662, and 1332 keV, respectively. These are in slightly better agreement with screened results as comparison with Table V indicates.

[10] S. Hultberg, Arkiv. Fysik **15**, 307 (1959).
[11] Z. Sujkowski, Arkiv Fysik **20**, 269 (1961).
[12] S. Colgate, Phys. Rev. **87**, 592 (1952).

TABLE VII. Ratio of total cross sections for the K and L shells of uranium. (1) Present work, (2) Alling and Johnson (Ref. 2).

ω (keV)	279	354	412	662	1000	1332
(1)	4.61	4.82	4.90	5.08	5.26	5.38
(2)	4.31	4.41	4.48	4.65	···	4.88

Total cross sections for the L shell have not been measured. Hultberg,[10] however, has measured the ratio σ_K/σ_L for uranium in the energy range 412 to 1332 keV. He finds the ratio to be essentially independent of energy and equal to 5.3 ± 0.2. Table VII gives this ratio from the new calculation as well as Alling and Johnson's unscreened results.[2]

The photon energies 81, 103, and 279 keV correspond to Sujkowski's[11] experimental energies for $Z=92$. He has measured the ratio $(\sigma_{L_{\mathrm{I}}}+\sigma_{L_{\mathrm{II}}})/\sigma_{L_{\mathrm{III}}}$ for 103 keV. His value is 3.03 ± 0.15. This is to be compared with the new result of 2.93 and the unscreened result of Alling and Johnson of 2.74. Figure 2 contains other experimental points[11,13] for this ratio and compares them with screened and unscreened predictions. It is hoped that future experiments will reduce the error bars. Sujkowski[11] has also measured the quantity $\sigma_{L_{\mathrm{II}}}/\sigma_{L_{\mathrm{III}}}$ for 81 keV and gives a value of 0.92 ± 0.15. The new result of 1.14 is in poorer agreement than Alling and Johnson's result of 1.08.

(C) Hartree Calculation

As a final check on the model, cross sections are computed for mercury, $Z=80$, at $\omega=354$ keV using relativistic Hartree wave functions and potentials.[14] The tabulated wave functions for the bound state are numerically interpolated. Corrections are made to the potential for the absence of the photoelectron and the tabulated values are fit to

$$V(r)=-(\alpha/r)[1+79(te^{-\lambda_1 r}+(1-t)e^{-\lambda_2 r})]. \quad (28)$$

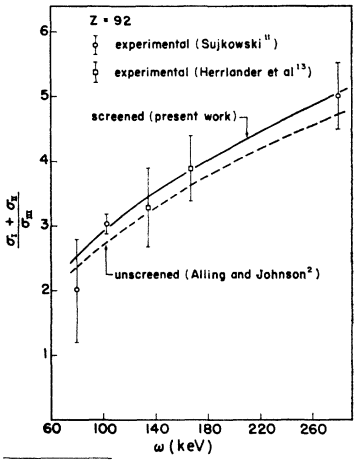

FIG. 2. Comparison of ratios of L-subshell cross sections computed using screened and unscreened wave functions with experiment.

[13] C. J. Herrlander, R. Stockendal, and R. K. Gupta, Arkiv. Fysik **17**, 315 (1960).
[14] D. F. Mayers, Proc. Roy. Soc. (London) **241**, 93 (1957).

TABLE VIII. Hartree potential parameters.

	K	L_{I}	L_{II}	L_{III}
t	0.7110	0.7795	0.7761	0.7789
λ_1	0.0202	0.0221	0.0220	0.0221
λ_2	0.1103	0.1555	0.1493	0.1533
λ	0.0458	0.0387	0.0401	0.0391

The values for t, λ_1, and λ_2 for the various shells are given in Table VIII. The screening parameter λ is included for comparison.

The single term potential model is an adequate representation of the Hartree potential in the bound-state region. The two disagree by about 1% at the location of the wave-function maximum. Since this region contributes the dominant portion to the radial integrals the model should predict screening effects reasonably accurately.

TABLE IX. Total cross section for $Z=80$, $\omega=354$ keV in barns.

	K	L_{I}	L_{II}	L_{III}
Coulomb	49.82	6.409	1.892	1.403
Screened	49.37	5.703	1.594	1.176
Hartree	49.1	5.73	1.57	1.10

Table IX lists the total cross sections computed. The estimated accuracy of the calculations using Hartree functions is 1–2%.

ACKNOWLEDGMENTS

The authors wish to acknowledge useful discussions with Dr. W. R. Alling and with Professor J. W. Mihelich. Thanks are also due to the Notre Dame Computing Center for extensive use of the UNIVAC-1107 computer.

APPENDIX

(*A*) *K and* L_{I} *shell:*

$$Q_x(\tfrac{1}{2})=[1/(2l+1)][I_{x,-1,l+1}-I_{x,-1,l-1}],$$
$$Q_x(-\tfrac{1}{2})=I_{x,1,l}+[1/(2l'+1)]\times[l'J_{x,1,l'-1}+(l'+1)J_{x,1,l'+1}].$$

(*B*) L_{II} *shell:*

$$Q_x(\tfrac{1}{2})=[1/(2l'+1)][J_{x,1,l'+1}-J_{x,1,l'-1}],$$
$$Q_x(-\tfrac{1}{2})=I_{x,1,l}+[1/(2l'+1)]\times[l'J_{x,1,l'-1}+(l'+1)J_{x,1,l'+1}].$$

(*C*) L_{III} *shell:*

$$Q_x(\tfrac{3}{2})=\frac{(3/2)^{1/2}}{(2l+3)(2l+1)(2l-1)}[(2l-1)I_{x,-2,l+2}-2(2l+1)I_{x,-2,l}+(2l+3)I_{x,-2,l-2}],$$

$$Q_x(\tfrac{1}{2})=\frac{(9/2)^{1/2}}{(2l+3)(2l+1)(2l-1)}[(l+2)(2l-1)I_{x,-2,l+2}-(2l+1)I_{x,-2,l}-(l-1)(2l+3)I_{x,-2,l-2}]+\frac{1}{(2)^{1/2}(2l'+1)}[J_{x,-2,l'+1}-J_{x,-2,l'-1}],$$

$$Q_x(-\tfrac{1}{2})=\frac{(9/2)^{1/2}}{(2l+3)(2l+1)(2l-1)}\Big[(l+1)(l+2)(2l-1)\times I_{x,-2,l+2}+\frac{2l(l+1)(2l+1)}{3}I_{x,-2,l}+(l-1)l(2l+3)I_{x,-2,l-2}\Big]+\frac{(2)^{1/2}}{(2l'+1)}\times[l'J_{x,-2,l'-1}+(l'+1)J_{x,-2,l'+1}],$$

$$Q_x(-\tfrac{3}{2})=\frac{(3/2)^{1/2}l(l+1)}{(2l+3)(2l+1)(2l-1)}[(l+2)(2l-1)I_{x,-2,l+2}-(2l+1)I_{x,-2,l}-(l-1)(2l+3)I_{x,-2,l-2}]+\frac{(3/2)^{1/2}l'(l'+1)}{(2l'+1)}[J_{x,-2,l'+1}-J_{x,-2,l'-1}].$$